SSRG International Journal of Electronics and Communication Engineering
ISSN: 2348-8549/ https://doi.org/10.14445/23488549/IJECE-V13I11P120

Volume 13 Issue 11, 330-341, November 2026
© 2026 Seventh Sense Research Group®

Original Article

An Effective Iris Biometric Model Segmentation and Classification using Improved Deep Learning Network

Nawaf Abdualaziz Almolhis

Department of Computer Science, College of Engineering and Computer Science, Jazan University, Jazan, Saudi Arabia.

Corresponding Author: naalmolhis@jazanu.edu.sa

Received: 15 September 2026 Revised: 16 October 2026 Accepted: 16 November 2026 Published: 27 November 2026

Abstract *- Iris biometrics is a new technology that attracted considerable research interest due to its challenges to identify individuals without physical touch. An automatic iris recognition system, however, is not so robust even when dealing with issues in illumination, image noise, eyelid and eyelash occlusion, specular reflection and variations in the pupil boundary and direction of look. These problems might render wrong segmentation of the iris region and lead to wrong iris information being extracted. In order to overcome the above-mentioned drawbacks, it is proposed an iris recognition system which includes image processing methods to reduce noise, iris segmentation, and iris classification technique. The proposed model detects the pupil boundary and outer iris boundary segmentation to segment the iris region accurately. For the segmentation of iris images of irises, subsequently, a modified Convolutional Neural Network (CNN) is used for the segmented images classification based on the architecture of AlexNet. Accuracies, precisions, recalls, and F1-scores are used for measuring the proposed model's performance. Also, the experimental results done show that the proposed model attains better performance than the existing models in iris recognition. The suggested framework boosts the dependability of iris-based biometric authentication and can be utilized for secure, contactless identification frameworks.*

Keywords *- Deep learning, Iris biometrics, Iris classification, Iris segmentation, Improved Convolutional Neural Network.*

1. Introduction

At present, human identities and authentication are the most critical ones. This is caused by external identity sources like magnetic interface cards and identity with Radio Frequency Identification (RFID) function. Possible internal clues to human identity could be in the iris, sclera, lip-form, nose shape, ear shape, palm, and face. The proposed system identifies and extracts iris ROI region as a typical semantic segmentation method based on a U-Net model. The input eye image will be cropped to a smaller image based on the ROI that was "fitted" for the iris, and ROI for the iris will be provided.

In this paper, the iris recognition technique which utilizes digital (Localization) for locating Pupils in iris images for biometric authentication is discussed. The suggested design involves, firstly, discovering the pupil zone's ROI employing the semantic segmentation separation scheme and after that, the ROI is recognized using U-net. There has been a growing number of biometric driver's licenses and passports in recent years. Multi modal Biometric Recognition Structure is used by industry experts and researchers in security and requirement of the system to make it more resilient and secure. Another successful structure that has been reported on is the single mode biometric structure; however, this type of structure is vulnerable. The multi-modal system is selected by biometric experts. Another study gives application of DL based techniques in biometric applications.

The research objective is to overcome the problem of the low number of existing datasets, a problem that can affect the accuracy rate of the classifiers. Here, iris recognition problem is explored by employing a hybrid DL model and a simple CNN model.

In other cases, interactive learning is provided, which equates to an economical but effective solution. It offers an interactive U-Net for iris segmentation with a Squeeze Expand unit to lower the time required to train models and to enhance storage efficiency by eliminating the number of parameters it requires. Although Deep Learning (DL) methods have improved iris recognition, accurate segmentation remains challenging when eye images contain

This is an open access article under the CC BY-NC-ND license (http://creativecommons.org/licenses/by-nc-nd/4.0/)

reflections, noise, uneven illumination, and partial occlusion. Errors during segmentation can affect the extracted iris features quality and reduce classification performance. Existing works have examined segmentation and DL classification using diverse architectures.

However, when image quality varies across datasets, recognition performance, balancing segmentation accuracy, and computational requirements remain important challenges.

This work's main contribution is the addition of image preprocessing, Restricted Circular Hough Transform (RCHT)-based iris boundary localization, and AlexNet-based classification into a single recognition pipeline. Rather than presenting a new segmentation or Neural Network algorithm, the study examines how these established techniques can be combined to improve iris recognition performance.

The evaluation of the proposed framework uses four CASIA datasets. Also, its classification performance is compared with a conventional CNN baseline and previously reported methods. The results provide evidence of the potential benefits of the combined framework under the evaluated experimental conditions. Based on the above concerns, the following contributions to the research is conducted:

- The preprocessing of input dataset is firstly performed, and then the iris image segmentation is performed by the contour border algorithm.
- In this study, pre-trained CNN architecture is developed and evaluated for classification. Particularly, an improved CNN architecture that is based on the AlexNet architecture is employed.
- This enhanced CNN structure that is based on AlexNet, is used to boost the recognition accuracy of the proposed approach.
- To test the effectiveness of the proposed improved CNN model architecture derived from the AlexNet model, four different iris datasets from CASIA are used for testing.

For comparison with existing solutions, the f1-score, accuracy, precision and recall are the most important performance indicators. The results achieved prove that the proposed system can easily be adapted to different data sets, without impairing its high accuracy level.

The work organization is given, where section 2 gives some account of an existing investigation into a DL network approach to segmentation and classification of iris images. The proposed model details are discussed in section 3.

Section 4 provides information regarding the research findings and comments along with some limitations of the present study. Section 5 concludes the work.

2. Literature Review

Balashanmugam et al. 2023 [1] designed an iris recognition model using the regional features of iris and the classification of an iris by the DL network AlexNet. Hsiao et al. (2021) [2] integrated U-Net and EfficientNet to produce the best segmentation and recognition results of the iris; Hsiao and Fan (2021) [3] used U-Net based pupil positioning with EfficientNet to attain improved iris biometric recognition performance. Rafik and Boubaker (2020) [4] proposed a multimodal biometric system based on right and left iris with CNN.

To enhance the performance and achieve better accuracy in iris image recognition, Winston et al. (2022) [5] explored the usage of Hybrid Deep Convolutional Neural Models. Recently, S. Sardar et al. proposed an interactive deep-learning-based approach to accurately segment the iris [6]. Alwawi et al. (2022) [7] builds a DL algorithm for iris recognition with the aim of solving the problems of computational efficiency and recognition accuracy. Alay and Al-Baity (2020) [8] have proposed an Iris, Face and Finger-vein Multimodal DL based Biometric Recognition Framework.

Garea-Llano and Morales-Gonzalez in their work [9] proposed a video-based DL iris recognition system for evaluating the iris–pupil region quality. In attempt to tackle this, Jayanthi et al. (2021) [10] introduced an integrated DL framework for iris detection and recognition based on recognizing effective features. To have an efficient and reliable iris recognition method, Farouk et al. (2022) [11] came up with the idea of biometrics. Considering the enhancement in iris region segmentation for iris-based biometric recognition, Almutiry (2022) [12] proposed an efficient DL based iris segmentation algorithm.

Omran and AlShemmary (2020) [13] used deep CNN for automatic iris recognition. However, Brown 2022 [14] studied the deep face–iris recognition problem to investigate robust image segmentation and hyperparameter tuning. In post-mortem human iris images, DL-based iris segmentation technique was analyzed by Hossain et al., 2024, as discussed in [15], to see the applicability of iris biometrics under post-mortem pictures. In [16], Saleh and Menemencioğlu have studied how eye diseases negatively affect iris segmentation and recognition accuracy by transferring deep-learning methods to this domain. Gao and Bourlai (2024) [17] have designed a SwinIris Transformer-based iris recognition system and studied the architecture of Transformers for iris biometrics. Kayadibi et al. (2022) [18] proposed an eye-state recognition model with the aid of transfer learning based on the AlexNet architecture.

As a result of this, Wang et al. (2022) [19] proposed a lightweight iris segmentation network for achieving effective iris-region extraction. Hafner et al 2021 [20] gave for iris

recognition a DL-based feature extraction methods. To enhance the performance of biometric authentication, Prasanth et al. (2023) [21] fused the Iris and Periocular Biometric Data into a CNN model. DualSANet [22] is proposed by Yang et al., which uses dual spatial-attention network for enhancing iris recognition using attention-based feature learning. They have applied an effective iris segmentation method that was proposed by Jan and Min-Allah in 2020 [23] in dealing with noise images of iris.

Mathias et al. 2022 [24] came up with a unified automated technique for segmenting the pupil and iris from on-axis images of the eye. Garg et al., 2021 [25] proposed an efficient Human Identification system using iris recognition. To counter the replay and template attack problems in iris recognition, Gupta and Sehgal (2020) [26] proposed a histogram-based DL framework, called HsIrisNet. Gupta and Sehgal (2020) [27] have proposed an iris recognition system with selective frequency-domain features using a DL approach.

Soni et al. (2021) [28] blended the Hough transform with a Neural Architecture Search Network (NAS Network) for face recognition, which is called iris recognition. To improve the recognition performance of the iris, Sun et al. (2022) [29] proposed a multi-scale convolutional feature-fusion network by integrating local circular Gabor filters with it. Recently, Lei et al. (2022) [30] presented an attention-based meta-transfer-learning method to solve a problem known as few-shot iris recognition.

A highly effective non-cooperative iris recognition was achieved by Petrov and Minakova (2020) [31] using Daugman integro-differential operator. Last but not least, Sun et al. (2022) [32] proposed a DNN-based open-set iris recognition technique that enhances recognition accuracy in an unknown identity scenario. However, there are recent advances in DL that have greatly enhanced the performance of biometric recognition systems, especially in terms of achieving more accurate extraction of features, segmentation of the features and efficient classification.

The fusion of adversarial learning and biometric pattern recognition has shown promise for creating high-quality synthetic datasets that mitigate privacy concerns in healthcare while boosting the robustness of the models. Likewise, XAI is used in the processing of biometric data to make it transparent and interpretable, while maintaining recognition accuracy (Shankar et al. 2025) [34]. Deep Convolutional Neural Network architectures have not only successfully classified medical images but have also shown their efficacy in medical image classification systems operating on images, such as skin cancer detection using optimized CNN classifiers (Kumar et al. 2024) [35] and pneumonia diagnosis from chest x-ray images using the Vision Transformer (Singh et al. 2024) [36] techniques. Artificial neural networks have also been widely used for image classification applications, which usually serve as a solid base for intelligent visual recognition systems (Ramasamy et al. 2023) [37].

Furthermore, the sets of optimization techniques used in DL frameworks have helped to increase the classification accuracy in complex image classification-related tasks such as UAV scene classification with white shark optimization (Ravishankar et al. 2023) [38] and efficient Deep Convolutional Data Fusion Model for healthcare imaging (Khadidos et al. 2023) [39] through introducing attention mechanism features. Other DL frameworks with attention and recurrent/deep architectures have emerged as the most important ones in recognizing unusual human activities (Kumar et al. 2023) [40].

Furthermore, sophisticated image classification algorithms have been used effectively for analysis of hyperspectral images (Shitharth et al. 2022) [41], for thermal image-based fault diagnosis (Selvaraj et al. 2022) [42], and for optimized diagnosis of large number of intelligent cervical cancer using optimized Artificial Neural Networks (Devarajan et al. 2022) [43]. Additionally, successful application of DL in biomedical field is dominated by the Conv-based robust framework (Manoharan et al. 2022) [44] and recurrent neural network models (Ayub et al. 2022) [45], which were applied successfully for reducing the motion artefacts in the multi-contrast magnetic resonance images for enhanced image quality for clinical use.

The potential usefulness of VGG16-based CNNs in the context of IIDDs has also been demonstrated in the field of IIDDs (Althubiti et al. 2022) [46], and binary/ternary classification of complex cognitive tasks from bio-signals showed excellent performance using machine learning algorithms (Manoharan et al. 2022) [47]. These studies underscore the critical role of devised efficient DL architectures, attention mechanisms, explainable AI, and advanced image processing techniques in boosting the segmentation precision, image feature representation, and classification accuracy, thereby establishing a solid research foundation for the development of an effective iris biometric segmentation and classification model using improved DL networks.

As a whole, the reviewed studies established that DL, CNNs, Transfer learning, Attention mechanisms, Transformer models, feature fusion and advanced segmentation techniques have been able to markedly enhance the performance of iris recognition, while still issues which arise from image noise, illumination variations, occlusion, segmentation errors, non-cooperative conditions, and computational efficiency.

Table 1. Review on existing works

Papers and Authors	Method	Advantages	Limitations
Garea-Llano et al. [9]	DL-based video iris recognition with iris–pupil region quality assessment	Improves iris recognition by evaluating the quality of the iris–pupil region and supports video-based biometric identification	Performance may be affected by low-quality video frames, illumination variations, motion, and iris-region occlusion
Jayanthi et al. [10]	DL-based integrated framework for iris preprocessing, detection, segmentation, feature extraction, and recognition	Provides an integrated framework for accurate iris detection, segmentation, and recognition	Performance may depend on model parameters and dataset characteristics; however, this article has been retracted and should be used with caution
Farouk et al. [11]	Edge detection, iris segmentation, CNN, and Hamming Distance (HD)	Combines image-processing and DL techniques to improve feature extraction and iris classification across multiple datasets	The method involves multiple processing stages and may require additional evaluation for real-time applications
Almutiry et al. [12]	DL-based iris segmentation algorithm	Improves iris-region extraction and provides better segmentation performance for noisy and unconstrained iris images	Performance may be influenced by image quality, dataset diversity, and the availability of sufficient training data
Omran et al. [13]	Deep CNN using backpropagation and Adam optimization	Provides automated iris recognition with efficient feature learning and reduced recognition time	The performance may vary across different datasets and may depend on the quality and diversity of the training images

3. Proposed Methodology

The proposed iris recognition system involves three main stages: image pre-processing, iris segmentation and iris classification. In the first step, the input iris images are dedicated to pre-processing that enhances the image quality and minimize the effects of noise, illumination variations and unwanted visual artifacts.

Noise can be suppressed, and the important information concerning the iris edge is preserved by using a median filter. Besides, morphological operation like opening, closing and dilation are used to get rid of small unwanted regions, to fill gaps, improve relevant structures and to make the iris image more qualitative. This is done by image pre-processing, which generates a clean and apt image to realize their iris-related extraction precisely.

For pre-processing, the contours of the iris are first found by using contour border technique and the desired region of the iris is separated from the other eye parts (contours). The segmentation process also serves to minimize the effect of non-iris regions such as the eyelids, eyelashes, pupil area and background information.

High segmentation accuracy is critical since the proposed model's feature-learning and classification accuracy relies on the accuracy of the extracted iris region. The segmented images of the iris are then preprocessed and structured before going to the classification stage.

In the last stage, a better CNN architecture, derived from the popular AlexNet architecture, is used for classification of the segmented iris image. The CNN is automatically trained to learn meaningful features, discriminative from the segmented regions of the iris, using multiple convolutional, activation, fully connected and pooling layers. The iris-segmented datasets are used for training the model, and hyperparameter tuning is carried out to assist the learning process and overall classification performance. During training, hyperparameters are optimized, and many important hyperparameters like learning rate, batch size, epochs of training, optimizer, etc are optimized for model. The optimized hyper-parameters proposed and their effect as a model on performance are discussed in Results and Discussion section, are optimized during the training process. The optimized hyperparameter values and their influence on the model performance are presented in the Results and Discussion section. Finally, the proposed model is tested on various iris databases to check its robustness, reliability and generalization property for different images having different characteristics and acquired under varied imaging conditions. Evaluation metrics including accuracy, precision, recall and F1 score are used to assess the proposed model's performance. Comparisons between existing methods and the results of the experiments to validate the proposed image-processing, segmentation, and improved AlexNet-based classification framework are conducted. The overall workflow of the proposed Iris Recognition System is shown in Figure 1.

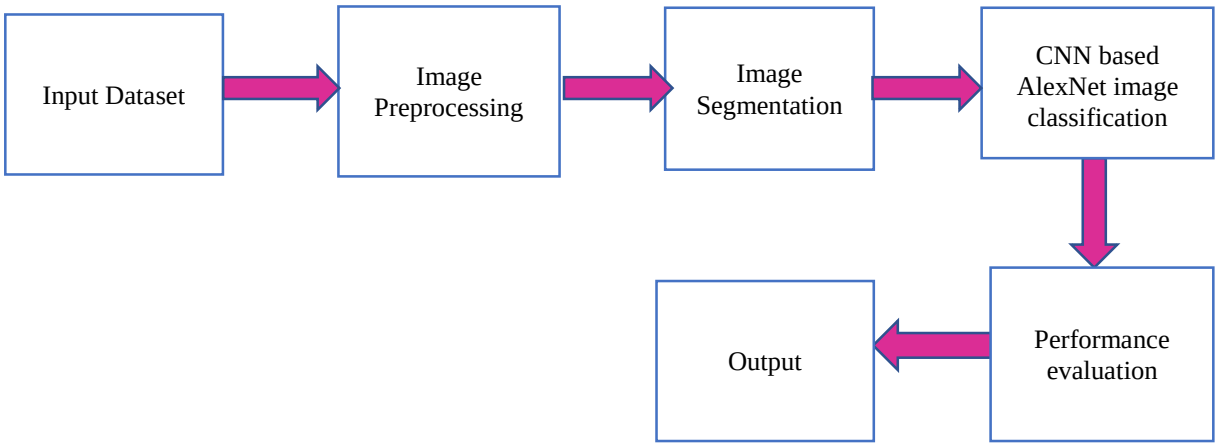

Fig. 1 Proposed architecture

3.1. Dataset Description

The CASIA datasets consist of benchmark datasets that are created and maintained by the Chinese Academy of Sciences Institute of Automation (CASIA). These datasets can be useful to a variety of fields such as handwritten character recognition, iris recognition, face recognition and so on. The three different datasets used are described.

- Conducted by CASIA, the CASIA IRIS Thousand dataset is comprised of images of the irises of 1,000 participants captured using IrisKing's IKEMB-100 cameras. IKEMB-100 is an iris camera designed with two eyes and ease of visual input. In the case of glasses, the main source of intra-class differences is specular reflections, as well as in CASIA-Iris-Thousand and CASIA-Iris-Stable. One thousand participants make CASIA-Iris-Thousand the publicly accessible dataset, making it ideal for research into iris characteristics' individuality and the creation of new iris classification methods.
- For CASIA-Iris-Interval versions 3 and 4, custom-built close-up iris camera has been utilized to capture images of iris. The most appealing
- The special feature of the iris camera is the circular array of NIR LEDs optimized so that the flux of light emitted by them will be best suited for iris imaging. Due to its unique design, iris camera can take pictures of the apparent iris.
- Data for the CASIA-Iris-Lamp dataset came from an OKI iris sensor that was portable. This switched the on/off of the light nearby, so as to increase the intra-class variability when collecting the CASIA-Iris-light. This dataset might be useful for the study of resilient iris feature representation and iris non-linear normalization.

Table 2. Datasets description

Name of the dataset	Class	Train	Testing	Total
CASIA-Iris-Thousand	1000	16000	4000	20000
CASIA-Iris-Lamp	411	12969	3243	16212
CASIA-Iris-Interval V3	249	2111	528	2639
CASIA-Iris- Interval V4	249	2111	528	2639

Table 2 gives a description about the datasets employed in this work. The CASIA-Iris-Thousand as well as CASIA-Interval datasets comprise respectively about 20,000 and 2639 images of the left and right eyes, respectively. While training, CASIA-Lamp used 12969 of its total, and for testing, 3243 of its total were used.

3.2. Image Pre-Processing

For this work, the pre-processing is done with aid of a median filter. Non-linearity can be represented as in equation (1) where Re_{pix} is the median value of the pixel. The letters "u" (for input), "n" (for another pixel that can be replaced), and "q" (for a term that can be tapped) are what are input into the image; "n" refers to a specific pixel, and "q" represents a specific term. In Equation (2), the filter tap detail is equal to "N", which represents a filter tap. Fixed thresholding method converts an image that is in grey scale to binary, the filter values are between 3 and 11. The expression for the fixed thresholding (3) is: if the input image is, for example, X, it has x (r, c), and if the input image is, for example, binary, it has y (r, c). The proposed one is based on filtering the image and converting it to binary form with image as input. The proposed method uses the same pupil threshold value (Thres), which is set to 127. If the threshold value is ≥ 127, then this program will add the logic value of "1" to the respective pixel.

$$Re_{pix}(n) = median_{pix}\begin{bmatrix} u(n-q), \\ u(n-q+1), \dots u(n), \\ \dots\dots, u(n+q-1), \\ u(n+q) \end{bmatrix} \quad (1)$$

$$q = \frac{(N-1)}{2} \quad (2)$$

$$y(r,c) = \begin{cases} 0 \; if \; or \; else \\ 1 \; if \; x(r,c) \geq Thres \end{cases} \quad (3)$$

In this work too, the morphological process comes into play for determination of the exact forms of the components using the mathematical functions. The next step was to use a pixel operation to shape the pixels. This step is applicable to both DILATION and EROSION. A very thin boundary over the structural element, due to erosion process. This made it look as if there were a thicker line up structural member when the dilation feature was used. Equation Processes (4) is an example of erosion, and (5) is an example of dilation. The single "Q" indicates a structured image ("Q" denotes structured), and the single "P" indicates an input image ("P" denotes input). In this example, x represents the basis of the vector 'Q_x'. Formal component begins with a 'Z'. Both the open and close operations are given by Equations (6) and (7), representing the morphological region. These either fill or delete structured pixels using open and closed regions. It can also apply the clean function and replace the 1s in the pixels that are close to the edge of the picture. Using Equations (4)-(8), the complement of this will come out to be the image's complement.

$$P \ominus Q = \{x \epsilon Z | Q_x \subseteq P\} \quad (4)$$

$$P \oplus Q = \cup_{q \epsilon Q} P_q \quad (5)$$

$$P \circ Q = (P \ominus Q) \oplus Q \quad (6)$$

$$P \cdot Q = (P \oplus Q) \ominus Q \quad (7)$$

$$\bar{P}(x,y) = 1 - P(x,y) \quad (8)$$

3.3. Iris Segmentation

Pre-processed iris images are used to perform segmentation on the Iris. After segmentation, iris image features are obtained, which is a very important step in Iris recognition. It ensures the accuracy of segmented iris image, since the segmented iris image is important in the classification process. The morphological procedures based on this segmentation approach were proposed. This research chose the segmentation algorithm as contour border algorithm.

The edges points used to identify the area of the iris are not even or rounded enough and are not adjoining each other to give us contours of the area. Using the RCHT of these edge points helps to fix the inside and outside of the iris area boundaries, the pupil-iris and Iris/Sclera boundaries, respectively. The RCHT approach, which is devised to narrow the search space, results in a faster CHT's computation time. Circular Hough transform (CHT) consists of advancing a 3-D accumulator cell (α, β, r); (x, y) increments the 3-D accumulator cell for the edge pixels.

$$r = \sqrt{(x-\alpha)^2 + (y-\beta)^2} \quad (9)$$

Where r is the radius, as well as (α, β) is the circle's presumed centre, for all α and all β. Finally, if there are all the image pixels, then the accumulator cell with the highest value is used to mark the radius and centre (x, y) of the circle. The effect of having large numbers (n>1) of accumulator C cells can be modelled as a quadratic surface containing only a single maximum taken in the (α, β, r) space. The value of the accumulated number is being monotonically decreased across the directions, and RCHT assumes that the cells having the largest accumulated value are presumed to be the surface maximum. The process begins by picking a first estimate (α, β) for the centre and then adds to the accumulator for all the image edge pixels for that centre. Records the highest value of accumulation.

The same process is performed after that at a set of symmetrically distributed locations at a distance d from and around (α, β) to consider these as possible centres. This is repeated until the centre with the highest cumulative value (i.e. the most total points) has done so. It cut the distance d in half and repeats the process if the new centre and old centre are the same. This is done repeatedly until (d = 0 (convergence. So, the RCHT is effective if the CHT is given in a small number of potential points (α, β). Please note that the first guess of the center is based on the locations of pixels on the edges of the "border image".

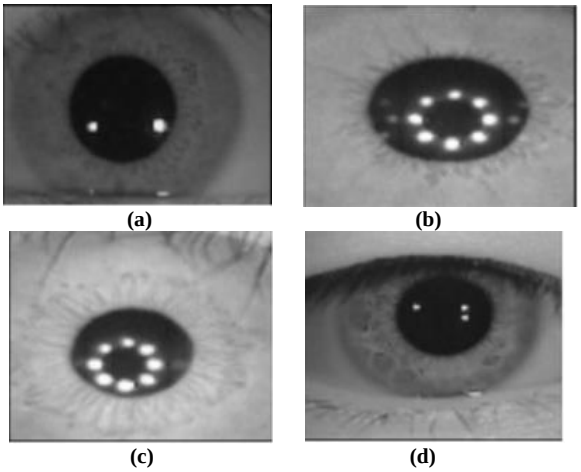

Fig. 2 Segmented iris image (a) CASIA-Iris-Thousand dataset, (b) CASIA-IntervalV3 dataset, (c) CASIA-IntervalV4 dataset, and (d) CASIA-Lamp dataset.

3.4. Iris Classification

The classification is done, followed by segmentation using the segmented images. Three fully connected layers as well as five convolutional layers comprise Alex-Net. There are multiple neurons in each convolutional layer, respectively. The minimal depth made the proposed architecture the chosen network over the other ones provided by Alex-Net. To do this, all layers had to be transferred to the new architecture, which was fully built using the transfer learning method, but in AlexNet, the FC8 fully connected layer was fully trained on the ImageNet dataset. Then, it enhanced the outputs with a finely tuned fully connected layer and dropped a fresh, randomly weighted fully connected layer into the design. This was named the newly constructed architecture-improved CNN-based AlexNet model. This compared the recommended architecture to evaluate its performance in the iris recognition approach that originally suggested its use of it instead of pre-trained designs.

Convolution layer: Grids of square numbers. These cores are used to convolution the input of the layer, creating and maintaining the value of the feature map. Firstly, the feature map is obtained in the kernel by propagating the input of the layer in the bottom-up direction and then in the left-right direction. In all dimensions, the following Equation (10) defines the convolution operation mathematical expression, which is the convolution of a continuous function x as well as w (x*w) (a):

$$(x * w)(a) = fx(t)w(a - t)da \qquad (10)$$

When n ≥ 1, then and = R^n. Furthermore, it replaces the higher-dimensional change integral by a change. But in reality, it is assumed that t is discrete, and the convolution for discrete parameters t is define by the following equation (11):

$$(x * w)(a) = \sum_a x(t)w(t - a) \qquad (11)$$

The feature map is obtained by mapping all the values in the input space as a travel over the entire input space, x is the input, and w is the kernel. The pooling layer is the next most important layer after the convolution layer. This layer highlights the proper ties in the picture, as well as attempts to reduce its size by collapsing areas where possible into one value. Activation Function Layer is a procedure that comes after the convolution layer. This function can be used to introduce non-linearity into DL models by providing instructions to the non-linear prediction bounds. In most CNNs, Rectified Linear Unit (ReLU) is utilized as the activation function.

It is followed by a normalising layer and other layers, after the convolution layer, the CNN is used. This layer normalizes the activations going through a network via gradients during training. Subsampling is usually accompanied by ReLU, pooling and normalisation layers. Additionally, after the convolution and subsampling layers, there is (at least) one fully connected layer.

Now this can be used to feed into feature maps with the fully connected layer using the softmax function. Normalization using softmax for the output of the fully connected layer. The last layer is classification layer, the loss function indicates the loss in this layer, and the closing of the softmax function indicates the assigned class.

To facilitate the pre-trained CNN architectures' training, the image processing enables the creation of dataset images in line with these specifications. The neurons count of the input layer was used to calculate the amount of resizing to use for each architecture.

The image size in the dataset was resized to fit the dimensions of the pre-trained CNN architectures used for training and test images in the dataset (227 × 227) for AlexNet. This led to the creation of the dataset, which will subsequently be used for testing and training. This processed two datasets this way, where they adjusted the input of the trained CNN models.

4. Results

The proposed system in the Jupiter environment uses a Windows 11 machine having 16 GB RAM, Intel Core i5 and, AlexNet model-based CNN architecture. It trained and tested all the employed architectures. The CNN training improvement architecture basically relies on the AlexNet CNN model, and an essential element of it is the hyper-parameter optimisation. The hyperparameters selected are explained in Table 3.

Table 3. Hyperparameters details

Parameter	Value
Optimizer	Nadam
L2 regularization	0.0001
Learning rate	0.0001
Loss criteria	Cross entropy
Gradient decay factor	0.9
epoch	20
Batch size	32

4.1. Performance Parameters

The segmented iris image shown in Figure 2(a) has been acquired from CASIA-Iris-Thousand database after training. The segmentation result of CASIA-IntervalV3 dataset is shown in Figure 2(b). The segmented image of iris, as shown in Figure 2(c), is from CASIA-IntervalV4 dataset. Result of segmentation from CASIA-Lamp dataset is shown in Figure 2(d). The results show that the proposed segmentation approach can successfully segment the iris area of images of various characteristics.

Using images from CASIA dataset, it was performed using the improved CNN-based AlexNet architectures. Then it created a confusion matrix on the basis of the results of the test results, and analyzed each architecture's performance. Based on this matrix, it calculated the Equations (12)-(15) for accuracy, sensitivity and precision:

$$accuracy = \frac{TP+TN}{FP+FN+TP+TN} \quad (12)$$

$$Sensitivity = \frac{TP}{(TP+FN)} \quad (13)$$

$$Precision = \frac{TP}{TP+FP} \quad (14)$$

$$F_1 score = 2 * \frac{precision*recall}{precision+recall} \quad (15)$$

TP, TN, FP and FN indicate true positive, true negative, false positive and false negative, respectively.

4.2. Discussion with CASIA Databases

The simple CNN will not be sufficient to achieve an acceptable accuracy, with first in the training of records. The CNN model without Alexnet, for example, got poor accuracy when training and testing the CASIA-Iris-Thousand dataset. Two different designs are compared using different sets in Table 5. This tests them with the f1-score, recall, accuracy and precision.

Table 4. Comparison of two architecture

Dataset name	Casia-Iris-Thousand	Casia-Iris-Intervalv3	Casia-Iris- Intervalv4	Casia-Iris-Lamp
CNN				
Accuracy	90.55	86.56	86.77	90.15
Precision	73.39	70.37	70.04	73.21
Recall	97.56	94.87	94.64	96.89
F1-score	83.77	80.31	80.36	82.78
CNN with Alexnet				
Accuracy	99.87	98.44	99.81	99.92
Precision	95.99	92.91	92.40	94.87
Recall	98.37	95.76	95.32	98.05
F1-score	97.67	94.79	94.65	97.14

Table 4 shows the comparison results when using two different architectures with the two sets of data. Using the CASIA-Iris-Thousand dataset, the proposed CNN with AlexNet method achieves excellent performance with a precision of 95.99%, recall of 98.37%, accuracy of 99.87% and F1-score of 97.67%. The CASIA IntervalV3 dataset has precision of 92.91%, recall of 95.76%, accuracy of 98.44%, and f1score of 94.79%. In the same manner, CASIA IntervalV4 dataset achieves 92.40% precision, 95.32% recall, 99.81% accuracy and 94.65% f1score. Finally, the CASIA-Iris-Lamp dataset has precision of 94.87%, recall of 98.05%, accuracy of 99.92%, and f1score of 97.14%.

The experimental results presented in Table 4 indicate that the proposed RCHT–AlexNet framework achieves higher recognition accuracy than the conventional CNN baseline across all four CASIA datasets. The improvements are 9.32, 11.88, 13.04, and 9.77 percentage points for CASIA-Iris-Thousand, CASIA-Iris-Interval V3, CASIA-Iris-Interval V4, and CASIA-Iris-Lamp, respectively.

One explanation for these improvements is the combination of iris-region localization and deep feature extraction. RCHT-based segmentation is intended to reduce the influence of non-iris regions by identifying the pupil and outer iris boundaries. The resulting iris regions are then processed by the AlexNet-based classifier, which learns discriminative image features for recognition.

Table 5. Testing accuracy on each dataset

Dataset	Accuracy
Casia-Iris-Intervalv3	98.44
Casia-Iris-Intervalv4	99.81
Casia-Iris-Lamp	99.92
Casia-Iris-Thousand	99.87

The higher accuracy observed across the evaluated datasets suggests that this combination may be beneficial for iris classification. However, the results do not independently establish the contribution of each processing stage. Additional controlled experiments would be necessary to determine how much of the improvement is attributable to segmentation, preprocessing, or the modified classifier.

Table 6 also compares the proposed approach with previously published methods. These results provide useful context for the reported recognition performance. Nevertheless, differences in subject counts, dataset partitions, preprocessing procedures, and evaluation protocols limit direct comparisons. Therefore, the reported results should be interpreted as evidence of competitive performance rather than definitive superiority over all existing approaches.

Table 6. Comparison with other existing approaches

Database	Authors	Method	Subjects	Accuracy
Casia-Iris-Thousand	Wang et al. [19], Hafner et al. [20], Prasanth et al. [21], Yang et al. [22], Proposed	Base-net DenseNet-201 CNN DualSANet CNN with AlexNet	100 1000 1000 1000 1000	99.66 98.5 99.23 99.64 99.87
Casia-Iris-Intervalv3	Jan et al. [23], Mathias et al. [24], Garg et al. [25], Proposed	- B-spline BPNN+GA CNN with AlexNet	121 249 50 249	99 94.60 96.40 98.44
Casia-Iris-Intervalv4	Gupta et al. [26], Gupta et al. [27], Soni et al. [28], Proposed	HsIrisNetCNN FrDIrisNet (CNN) Data-driven Gabor filter optimization CNN with AlexNet	373(L+R) 185 42 249	99.72 99.72 100 99.81
Casia-Iris-Lamp	Sun et al. [29], Lei et al. [30], Petrov et al. [31], J. Sun et al. [32], Proposed	MCFFN AttentionMTL Daugman integro-differential operator OCFON CNN with AlexNet	100 200 - 275 411	98.62 92.81 79 98.50 99.92

Table 5 presents the results of the accuracy analyses of the proposed approach. The accuracy ranges from 98.44%, 98.81%, 99.92%, as well as 99.81% for CASIA IntervalV3, CASIA IntervalV4, CASIA-Iris-Lamp and CASIA-Iris-Thousand. The results obtained on comparing different Iris recognition methods in the datasets applied in this study are shown in Table 6.

4.3. Limitation

By aiming to examine thoroughly, investigate and communicate openly, it is essential to consider the constraints of the work, particularly in the context of image processing of the iris. This found that it is segmenting/recognising some of the pre-processed images incorrectly. That is, when looking for eyes, some images of the eyes in the image result in the capturing of a bounding box (or a circle) and not an eyeball. The lack of the pupillary area in the centre of the false segmented image might pose another bottleneck for feature extraction, resulting in loss of some iris features. All of these may have a potential impact on the accuracy of the iris recognition system in the long term. Moreover, it is assumed that this study does not consider the temporal complexity.

Although the proposed method achieves high recognition accuracy on the evaluated CASIA datasets, the experimental results are subject to certain limitations. The comparison with previously published approaches does not use identical experimental conditions, and therefore direct conclusions about superiority should be made cautiously. Further evaluation using additional datasets, repeated experiments, and controlled comparisons would provide stronger evidence of the robustness and generalization ability of the proposed framework.

5. Conclusion

The proposed iris recognition system is developed based on CNN-based Alexnet, with a very high validated accuracy between 95% and 99% to accurately recognize the iris patterns automatically. It is high in comparison with other methods with various datasets, ranging from 95% to 99% accuracy. Using DL in biometric recognition has been validated in this performance, as an outcome of the sophisticated architecture tested. Based on the experiments, CNN and CNN with Alexnet designs seem to differ in terms of accuracy.

From the context of; training accuracy, testing accuracy, the CNN with Alexnet model achieved good results compared to the first CNN model. The proposed method also improves the accuracy when compared with the current state-of-the-art. Future studies could seek to improve and modernize iris detection and segmentation techniques, as they are not very suitable for very large-scale datasets. It is, however, noteworthy to point out that this paper used an automated iris detection and segmentation process that saved a considerable amount of time.

Funding Statement

There was no external funding for this study.

Data Availability Statement

The data is made public at this link: https://www.kaggle.com/datasets/swoyam2609/casia-iris-interval. Details of data are provided in this article.

Conflicts of Interest

The authors have no conflicts of interest to declare.

References

[1] Thiyaneswaran Balashanmugam et al., "An Effective Model for the Iris Regional Characteristics and Classification Using Deep Learning Alex Network," *IET Image Processing*, vol. 17, no. 1, pp. 227-238, 2023. [CrossRef] [Google Scholar] [Publisher Link]

[2] Cheng-Shun Hsiao, Chih-Peng Fan, and Yin-Tsung Hwang, "Design and Analysis of Deep-Learning-based Iris Recognition Technologies by Combination of U-Net and EfficientNet," *2021 9th International Conference on Information and Education Technology (ICIET)*, Okayama, Japan, pp. 433-437, 2021. [CrossRef] [Google Scholar] [Publisher Link]

[3] Cheng-Shun Hsiao, and Chih-Peng Fan, "EfficientNet-based Iris Biometric Recognition Methods with Pupil Positioning by U-Net," *2021 3rd International Conference on Computer Communication and the Internet (ICCCI)*, Nagoya, Japan, pp. 1-5, 2021. [CrossRef] [Google Scholar] [Publisher Link]

[4] Hammou Djalal Rafik, and Mechab Boubaker, "A Multi-Biometric System based on the Right Iris and the Left Iris Using the Combination of Convolutional Neural Networks," *2020 Fourth International Conference On Intelligent Computing in Data Sciences (ICDS)*, Fez, Morocco, pp. 1-10, 2020. [CrossRef] [Google Scholar] [Publisher Link]

[5] J. Jenkin Winston et al., "Hybrid Deep Convolutional Neural Models for Iris Image Recognition," *Multimedia Tools and Applications*, vol. 81, pp. 9481-9503, 2022. [CrossRef] [Google Scholar] [Publisher Link]

[6] Mousumi Sardar, Subhashis Banerjee, and Sushmita Mitra, "Iris Segmentation using Interactive Deep Learning," *IEEE Access*, vol. 8, pp. 219322-219330, 2020. [CrossRef] [Google Scholar] [Publisher Link]

[7] Bashra Kadhim Oleiwi Chabor Alwawi, and Ali Fadhil Yaseen Althabhawee, "Towards More Accurate and Efficient Human Iris Recognition Model using Deep Learning Technology," *TELKOMNIKA (Telecommunication Computing Electronics and Control)*, vol. 20, no. 4, pp. 817-824, 2022. [CrossRef] [Google Scholar] [Publisher Link]

[8] Nada Alay, and Heyam H. Al-Baity, "Deep Learning Approach for Multimodal Biometric Recognition System based on Fusion of Iris, Face, and Finger Vein Traits," *Sensors*, vol. 20, no. 19, pp. 1-17, 2020. [CrossRef] [Google Scholar] [Publisher Link]

[9] Eduardo Garea-Llano, and Annette Morales-Gonzalez, "Framework for Biometric Iris Recognition in Video, by Deep Learning and Quality Assessment of the Iris-Pupil Region," *Journal of Ambient Intelligence and Humanized Computing*, vol. 14, no. 6, pp. 6517-6529, 2023. [CrossRef] [Google Scholar] [Publisher Link]

[10] J. Jayanthi et al., "An Effective Deep Learning Features-based Integrated Framework for Iris Detection and Recognition," *Journal of Ambient Intelligence and Humanized Computing*, vol. 12, no. 3, pp. 3271-3281, 2021. [CrossRef] [Google Scholar] [Publisher Link]

[11] Rahmatallah Hossam Farouk, Heba Mohsen, and Yasser M. Abd El-Latif, "A Proposed Biometric Technique for Improving Iris Recognition," *International Journal of Computational Intelligence Systems*, vol. 15, no. 1, pp. 1-11, 2022. [CrossRef] [Google Scholar] [Publisher Link]

[12] Omar Almutiry, "Efficient Iris Segmentation Algorithm using Deep Learning Techniques," *Journal of Electronic Imaging*, vol. 31, no. 4, 2022. [CrossRef] [Google Scholar] [Publisher Link]

[13] Maryim Omran, and Ebtesam N. AlShemmary, "An Iris Recognition System using Deep Convolutional Neural Network," *Journal of Physics: Conference Series*, vol. 1530, no. 1, pp. 1-11, 2020. [CrossRef] [Google Scholar] [Publisher Link]

[14] Dane Brown, "Deep Face-Iris Recognition using Robust Image Segmentation and Hyperparameter Tuning," *Computer Networks and Inventive Communication Technologies: Proceedings of Fourth ICCNCT 2021*, pp. 259-275, 2022. [CrossRef] [Google Scholar] [Publisher Link]

[15] Afzal Hossain, Tipu Sultan, and Stephanie Schuckers, "Post-Mortem Human Iris Segmentation Analysis with Deep Learning," *arXiv Preprint*, pp. 1-9, 2024. [CrossRef] [Google Scholar] [Publisher Link]

[16] Abbadullah .H Saleh, and Oğuzhan Menemencioğlu, "Study the Effect of Eye Diseases on the Performance of Iris Segmentation and Recognition using Transfer Deep Learning Methods," *Engineering Science and Technology, an International Journal*, vol. 47, pp. 1-11, 2023. [CrossRef] [Google Scholar] [Publisher Link]

[17] Runqing Gao, and Thirimachos Bourlai, "On Designing a SwinIris Transformer-based Iris Recognition System," *IEEE Access*, vol. 12, pp. 30723-30737, 2024. [CrossRef] [Google Scholar] [Publisher Link]

[18] Ismail Kayadibi et al., "An Eye State Recognition System using Transfer Learning: AlexNet-based Deep Convolutional Neural Network," *International Journal of Computational Intelligence Systems*, vol. 15, no. 1, pp. 1-19, 2022. [CrossRef] [Google Scholar] [Publisher Link]

[19] Qi Wang et al., "A Light Iris Segmentation Network," *The Visual Computer*, vol. 38, no. 7, pp. 2591-2601, 2022. [CrossRef] [Google Scholar] [Publisher Link]

[20] Andrej Hafner et al., "Deep Iris Feature Extraction," *2021 International Conference on Artificial Intelligence in Information and Communication (ICAIIC)*, Jeju Island, Korea (South), pp. 258-262, 2021. [CrossRef] [Google Scholar] [Publisher Link]

[21] Nalluri Prasanth et al., "Fusion of Iris and Periocular Biometrics Authentication using CNN," *2023 7th International Conference on Computing Methodologies and Communication (ICCMC)*, Erode, India, pp. 378-382, 2023. [CrossRef] [Google Scholar] [Publisher Link]

[22] Kai Yang, Zihao Xu, and Jingjing Fei, "DualSANet: Dual Spatial Attention Network for Iris Recognition," *2021 IEEE Winter Conference on Applications of Computer Vision (WACV)*, Waikoloa, HI, USA, pp. 888-896, 2021. [CrossRef] [Google Scholar] [Publisher Link]

[23] Farmanullah Jan, and Nasro Min-Allah, "An Effective Iris Segmentation Scheme for Noisy Images," *Biocybernetics and Biomedical Engineering*, vol. 40, no. 3, pp. 1064-1080, 2020. [CrossRef] [Google Scholar] [Publisher Link]

[24] Grissel Priyanka Mathias et al., "A Unified Approach for Automated Segmentation of Pupil and Iris in On-Axis Images," *Computer Methods and Programs in Biomedicine Update*, vol. 2, pp. 1-11, 2022. [CrossRef] [Google Scholar] [Publisher Link]

[25] Mamta Garg, Ajatshatru Arora, and Savita Gupta, "An Efficient Human Identification through Iris Recognition System," *Journal of Signal Processing Systems*, vol. 93, no. 6, pp. 701-708, 2021. [CrossRef] [Google Scholar] [Publisher Link]

[26] Richa Gupta, and Priti Sehgal, "HsIrisNet: Histogram-based Iris Recognition to Allay Replay and Template Attack using Deep Learning Perspective," *Pattern Recognition and Image Analysis*, vol. 30, no. 4, pp. 786-794, 2020. [CrossRef] [Google Scholar] [Publisher Link]

[27] Richa Gupta, and Priti Sehgal, "Iris Recognition using Selective Feature Set in Frequency Domain using Deep Learning Perspective: FrDIrisNet," *Cybernetics, Cognition and Machine Learning Applications: Proceedings of ICCCMLA*, pp. 249-259, 2020. [CrossRef] [Google Scholar] [Publisher Link]

[28] Ashutosh Soni et al., "Iris Recognition using Hough Transform and Neural Architecture Search Network," *2021 Innovations in Power and Advanced Computing Technologies (i-PACT)*, Kuala Lumpur, Malaysia, pp. 1-5, 2021. [CrossRef] [Google Scholar] [Publisher Link]

[29] Jie Sun et al., "Iris Recognition Based on Local Circular Gabor Filters and Multi-Scale Convolution Feature Fusion Network," *Multimedia Tools and Applications*, vol. 81, no. 23, pp. 33051-33065, 2022. [CrossRef] [Google Scholar] [Publisher Link]

[30] Songze Lei et al., "Attention Meta-Transfer Learning Approach for Few-Shot Iris Recognition," *Computers and Electrical Engineering*, vol. 99, 2022. [CrossRef] [Google Scholar] [Publisher Link]

[31] I. Petrov, and N. Minakova, "Optimization Method for Non-Cooperative Iris Recognition Task using Daugman Integro-Differential Operator," *Journal of Physics: Conference Series*, vol. 1615, no. 1, pp. 1-10, 2020. [CrossRef] [Google Scholar] [Publisher Link]

[32] Jie Sun et al., "Open-Set Iris Recognition based on Deep Learning," *IET Image Processing*, vol. 16, no. 9, pp. 2361-2372, 2022. [CrossRef] [Google Scholar] [Publisher Link]

[33] Adil O. Khadidos et al., "Synthetic Healthcare Data Utility with Biometric Pattern Recognition using Adversarial Networks," *Scientific Reports*, vol. 15, pp. 1-19, 2025. [CrossRef] [Google Scholar] [Publisher Link]

[34] Achyut Shankar et al., "Transparency and Privacy Measures of Biometric Patterns for Data Processing with Synthetic Data Using Explainable Artificial Intelligence," *Image and Vision Computing*, vol. 154, 2025. [CrossRef] [Google Scholar] [Publisher Link]

[35] Ashwani Kumar et al., "A Novel Skin Cancer Detection Model using Modified Finch Deep CNN Classifier Model," *Scientific Reports*, vol. 14, pp. 1-19, 2024. [CrossRef] [Google Scholar] [Publisher Link]

[36] Sukhendra Singh et al., "Efficient Pneumonia Detection using Vision Transformers on Chest X-rays," *Scientific Reports*, vol. 14, pp. 1-17, 2024. [CrossRef] [Google Scholar] [Publisher Link]

[37] Jayaraj Ramasamy, R. N. Ravikumar. and S. Shitharth, *Artificial Neural Networks for Data Processing: A Case Study of Image Classification*, Advances in Mathematical Applications in Data Science, pp. 116-127, 2023. [CrossRef] [Google Scholar] [Publisher Link]

[38] T. Nadana Ravishankar et al., "White Shark Optimizer with Optimal Deep Learning based Effective Unmanned Aerial Vehicles Communication and Scene Classification," *Scientific Reports*, vol. 13, pp. 1-19, 2023. [CrossRef] [Google Scholar] [Publisher Link]

[39] Alaa O. Khadidos et al., "TasLA: An Innovative Tasmanian and Lichtenberg Optimized Attention Deep Convolution-based Data Fusion Model for IoMT Smart Healthcare," *Alexandria Engineering Journal*, vol. 79, pp. 337-353, 2023. [CrossRef] [Google Scholar] [Publisher Link]

[40] Manoj Kumar et al., "Attention-Based Bidirectional-Long Short-Term Memory for Abnormal Human Activity Detection," *Scientific Reports*, vol. 13, pp. 1-12, 2023. [CrossRef] [Google Scholar] [Publisher Link]

[41] Shitharth S et al., "Hyperspectral Image Classifications for Monitoring Harvests in Agriculture using Fly Optimization Algorithm," *Computers and Electrical Engineering*, vol. 103, 2022. [CrossRef] [Google Scholar] [Publisher Link]

[42] Tamilselvi Selvaraj et al., "Environmental Fault Diagnosis of Solar Panels using Solar Thermal Images in Multiple Convolutional Neural Networks," *International Transactions on Electrical Energy Systems*, vol. 2022, no. 1, pp. 1-16, 2022. [CrossRef] [Google Scholar] [Publisher Link]

[43] Devikanniga Devarajan et al., "Cervical Cancer Diagnosis using Intelligent Living Behaviour of Artificial Jellyfish Optimized with an Artificial Neural Network," *IEEE Access*, vol. 10, pp. 126957-126968, 2022. [CrossRef] [Google Scholar] [Publisher Link]

[44] Hariprasath Manoharan et al., "A Machine Learning Algorithm for Classification of Mental Tasks," *Computers and Electrical Engineering*, 2022. [CrossRef] [Google Scholar] [Publisher Link]

[45] Shahanaz Ayub et al., "LSTM-based RNN Framework to Remove Motion Artifacts in Dynamic Multi-Contrast MR Images with Registration Model," *Wireless Communications and Mobile Computing*, vol. 2022, no. 1, pp. 1-12, 2022. [CrossRef] [Google Scholar] [Publisher Link]

[46] Sara A. Althubiti et al., "Circuit Manufacturing Defect Detection using VGG16 Convolutional Neural Networks," *Wireless Communications and Mobile Computing*, vol. 2022, no. 1, pp. 1-10, 2022. [CrossRef] [Google Scholar] [Publisher Link]

[47] Hariprasath Manoharan et al., "Deep Conviction Systems for Biomedical Applications using Intuiting Procedures with Cross Point Approach," *Frontiers in Public Health*, vol. 10, pp. 1-14, 2022. [CrossRef] [Google Scholar] [Publisher Link]